Hindawi Publishing Corporation
Journal of Applied Mathematics
Volume 2014, Article ID 624863, 13 pages
http://dx.doi.org/10.1155/2014/624863

Research Article

Constitutive Relation of Engineering Material Based on SIR Model and HAM

Haoxiang He, Enzhen Han, and Maolin Cong

Beijing Laboratory of Earthquake Engineering and Structural Retrofit, Beijing University of Technology, Beijing 100124, China

Correspondence should be addressed to Haoxiang He; hhx7856@163.com

Received 7 March 2014; Revised 20 May 2014; Accepted 1 June 2014; Published 22 June 2014

Academic Editor: Xiaojing Yang

As an epidemic mathematical model, the SIR model represents the transition of the Susceptible, Infected, and Recovered. The profound implication of the SIR model is viewed as the propagation and dynamic evolutionary process of the different internal components and the characteristics in a complex system subject to external effect. The uniaxial stress-strain curve of engineering material represents the basic constitutive relation, which also represents the damage propagation in the units of the damaged member. Hence, a novel dynamic stress-strain model is established based on the SIR model. The analytical solution and the approximate solution for the proposed model are represented according to the homotopy analysis method (HAM), and the relationship of the solution and the size effect and the strain rate is discussed. In addition, an experiment on the size effect of confined concrete is carried out and the solution of SIR model is suitable for simulation. The results show that the mechanical mechanism of the parameters of the uniaxial stress-strain model proposed in this paper reflects the actual characteristics of the materials. The solution of the SIR model can fully and accurately show the change of the mechanical performance and the influence of the size effect and the strain rate.

1. Introduction

Engineering material means the material used for engineering or the materials used to produce other materials which may be used in engineering. The traditional material in civil engineering includes concrete, steel, soil, wood, and alloy. These materials have different qualities about strength, workability, durability, and resistance against corrosion [1]. The materials differ also in their structure, texture, and performance. The strength, toughness, and ductility of construction material are the fundamental guarantee for engineering reliability. With the development of civil engineering, the type and form of civil engineering materials are unceasingly rich and the performance is enhanced also, and the corresponding research and application on experimental techniques, theoretical analysis, numerical simulation, and actual engineering are improved constantly. However, there are still more phenomena to be interpreted and more research issues should be given attention because the engineering material has microcrack, heterogeneity, and evolution in micromechanics and shows elastoplasticity, discreteness, and randomness in the micromechanics. In addition, the mechanical behaviors of engineering materials are also related to the size, the loading rate, the external environment, and other factors. Therefore, the mechanical properties of different engineering materials have obvious differences; the demand about the experiment and numerical simulation for various materials are diverse. Researchers normally investigate the mechanic property of the specified material, and the study on the generalized characteristics for various construction materials is still not intense.

The uniaxial stress-strain curve indicates the simple mechanic property of the material subjected to pure compress or pure tension; representing the basic material constitutive relation and the uniaxial stress-strain relation is also the foundation to establish multiple compound constitutive models. In the elastoplasticity or nonlinear analysis, the uniaxial stress-strain curve plays a decisive role in the accuracy of the numerical results. Furthermore, the computational analysis of the engineering structure subjected to dynamic or cyclic loadings requires the stress-strain models to simulate the response of the structure [2, 3].

There are many types of stress-strain curves models for different material or even one kind of material. As known to all, the stress-strain curve of concrete has a variety of forms or functions because concrete is a type of composite material and the discreteness is obvious. Numerous concrete models have been proposed in the last years. For example, the compressive stress-strain function for concrete consists of five kinds of equations as polynomial, exponential, and trigonometric function, rational fraction, and sectional form and the total number of the corresponding formulas is over 20 [2].

In the macroscopic level, three broad categories can be distinguished: models derived from the theory of elasticity, models based on the theory of plasticity, and models based on the continuum damage theory [3, 4]. Also, some coupled models based on the association of plasticity and continuum damage theory have been recently developed. Although it has been proved that the models derived from theory of plasticity and continuum damage theory can accurately simulate the observed behavior of concrete, the engineering application of these models is less. This is motivated by the great amount of parameters that are usually needed and the difficulty to obtain them through conventional laboratory tests. From the perspective of another point of view, the structural member with definite shape and materials is a complex system which has huge amounts of units, and the units have the whole process of sustained force, damage, interact, transmitting energy, and propagation, until failure. The characteristics of all the units generally constitute the property of the macromaterial and member.

Hence, taking the damage propagation and transmit in the microunits into consideration, establishing a new and generalized uniaxial constitutive model which can take into account that both the versatility and the dirigibility is necessary.

2. SIR Model and Its Connection between Constitutive Relations of Material

An epidemic represents the sudden outbreak and propagation of a disease, often occurring on a short temporal scare and affecting a significant portion of a population. Epidemics also may exhibit some periodic behavior, as opposed to endemics, which are diseases that are always present to some extent in a population. Epidemiology is the branch of science which essentially deals with the mathematical modeling of propagation of diseases. The first mathematical model of epidemiology was formulated and solved by Daniel Bernoulli in 1760. Kermack and McKendrick [5] illustrated that diseases showed a threshold type of behavior. In other words, if a single person infected by a particular disease passed on the infection to more than one person in turn, an epidemic would occur, while if less than one secondary infection occurred in each primary one, the disease would die out. The study of mathematical epidemiology has grown rapidly, with a large variety of models having been formulated and applied to infectious diseases. The epidemic model can describe the dynamic process of the epidemic, and spread characteristics will be grasped based on the information of the change of population; then the epidemic can be effectively controlled. The general epidemic model belongs to first order ordinary differential equations, and the most representative is the SIR model.

The SIR epidemic mathematical model is presented based on a system of first order ordinary differential equations and it has been used in the modeling of several infectious diseases, where the parameters need to be estimated by epidemiological data [6]. In this model, the variables represent subpopulations of the Susceptible (S) who can catch the disease, the Infected (I) who are infected and can transmit the disease to the Susceptible, and the Removal (R) who had the disease and recovered or died or have developed immunity or have been removed from contact with the other classes. Thus, the model describes the propagation and transformation between different classes. Assume that the total number of population is one unit for the sake of simplicity and the SIR model is written as

$$\begin{aligned} \frac{di(t)}{dt} &= \lambda i(t) s(t) - \mu i(t), \\ \frac{ds(t)}{dt} &= -\lambda i(t) s(t) + \eta i(t) - \rho i^2(t) s(t), \end{aligned} \tag{1}$$

where $i(t)$ and $s(t)$ denote the Infected and the Susceptible, respectively, and $r(t)$ is Removal and t is time. Hence, $s(t) + i(t) + r(t) = 1$ is satisfied. λ is the infectivity coefficient of the typical Lotka-Volterra interaction term, which means the daily contact rate (i.e., the population that each patient effectively contact with the healthy persons every day). μ is the daily recovery rate or number of patients cured or removed out accounting for the proportion of the total patients. η is the increasing rate of Susceptible persons when patients are increasing. ρ is the speed parameter after taking preventive and control measures. The SIR model is subject to the initial conditions $i(0) = i_0$ and $s(0) = s_0$, where $i_0 > 0$ and $s_0 > 0$ are given constants.

From the introduction above, it is significant that the SIR model is not simply an equation representing the spread of an epidemic, while it actually describes the propagation and dynamic evolution process of the different internal components and the characteristics in a complex system subject to external effect. In general, the SIR model embodies the general characteristics and rules in the similar system with propagation and transformation. The continuous damage and destruction will occur for the material specimen in civil engineering under increasing load, and the unstressed units, the stressed units, and the fractured or invalid units in anyone state should be included. The stress-strain relationship is the typical representation of the propagation and the dynamic evolution. Therefore, an innovative model for the material can be presented referencing to the SIR model, and the two models have similar parameters. To validate this interpretation, a compressed concrete specimen with 60 mm diameter and 120 mm height is selected as an example. The uniaxial failure process of the specimen is simulated based on the three-dimensional mesolevel finite element method [7, 8], and the failure charts in different stage are shown in Figure 1.

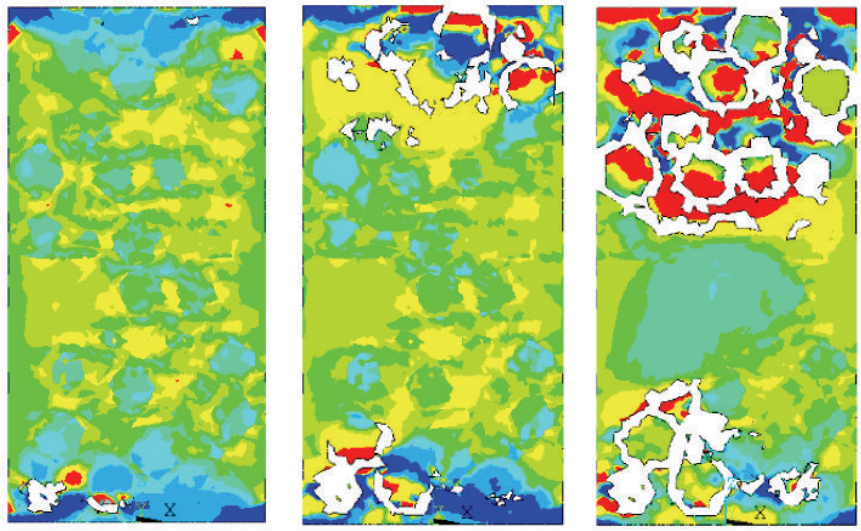

FIGURE 1: Damage propagation process and different units based on microlevel simulation.

It is clear that there are unstressed units, stressed units, and the fractured or invalid units in all stages, whereas the damage propagation and the proportion of each part are time-variant. The unstressed units are majority and fractured units are few at the initial stage. With the compression being enhanced, the units participate in the resistance gradually and the stressed units boom. After the counteragent in most units decreases, the invalid units increase and the cracks appear, though the stressed units decline and the specimen collapses. In conclusion, the SIR model is suitable for illustrating the failure process of materials, that is, typical damage propagation process in a complex system.

Strain ε reflects the deformation capability and damage process of material, corresponding with the time variable t in the SIR model. $s(\varepsilon)$, $\sigma(\varepsilon)$, and $r(\varepsilon)$ represent the equivalent stress in unstressed units, the equivalent stress in stressed units, and the equivalent stress in fractured or invalid units, respectively. This model subjects to the initial conditions $\sigma(0) = \sigma_0$ and $s(0) = s_0$, where $\sigma_0 > 0$ and $s_0 > 0$ are given constants. In the same manner, $s(\varepsilon) + \sigma(\varepsilon) + r(\varepsilon) = 1$. In this case, λ can be viewed as the transmissibility rate in units, and μ represents the failure rate in units. η can be expressed as the increase rate of stressed units when the invalid units grow, and ρ is the reduced speed parameter for invalid units due to stress transmission and distribution. Finally, the stress-strain model of material can be expressed as

$$\begin{aligned} \frac{d\sigma(\varepsilon)}{d\varepsilon} &= \lambda\sigma(\varepsilon)\, s(\varepsilon) - \mu\sigma(\varepsilon), \\ \frac{ds(\varepsilon)}{d\varepsilon} &= -\lambda\sigma(\varepsilon)\, s(\varepsilon) + \eta\sigma(\varepsilon) - \rho\sigma^2(\varepsilon)\, s(\varepsilon). \end{aligned} \tag{2}$$

Equation (2) is nonlinear differential equations which represent the coupling and transformation of the three types of units and the full complex process for the material from intact to failure. The system of equations has the unique solution, but the analytical solution cannot be obtained by normal mathematical methods and the results are calculated usually by numerical methods.

Assume the basic condition of the equation above is that λ is 1.00, μ is 0.15, η is 0.1, ρ is 0.8, and $\sigma(0)$ is 0.02. The consequences of the equivalent stress $\sigma(\varepsilon)$ under different parameters are solved by numerical method, as shown in Figure 2. It is obvious that the full curves accurately indicate the linear ascent stage, nonlinear yield stage, and the decline stage or strengthening stage after peak stress. Further, the variation of μ, η, or ρ can obviously affect peak and ductility of the stress-strain curve, and different forms of the curve can be obtained according to the overall adjustment of the corresponding parameters.

Different solutions of SIR model in various conditions can represent the stress-strain curves of diverse types of materials. Figure 3 reveals the stress-strain curves including concrete or rock-soil in compression or tension as well as different types of stress-strain curves of soils and steel obtained by numerical methods. The comparison curves of the real experimental data and numerical solution about the concrete and steel are shown in Figures 4 and 5, respectively. In order to compare the regularity but not the specific data, the peak strain is normalized. By changing the parameter appropriately, the full stress-strain curve obtained from (2) can simulate the peak stress, ductility, and softening stage of concrete with different strength, as shown in Figure 6. The results above show that the SIR model can really represent different mechanical properties of materials generally. It is worth noting that the initial values of the curves obtained by (2) are adjusted to the origin of coordinate and the coordinate values only have

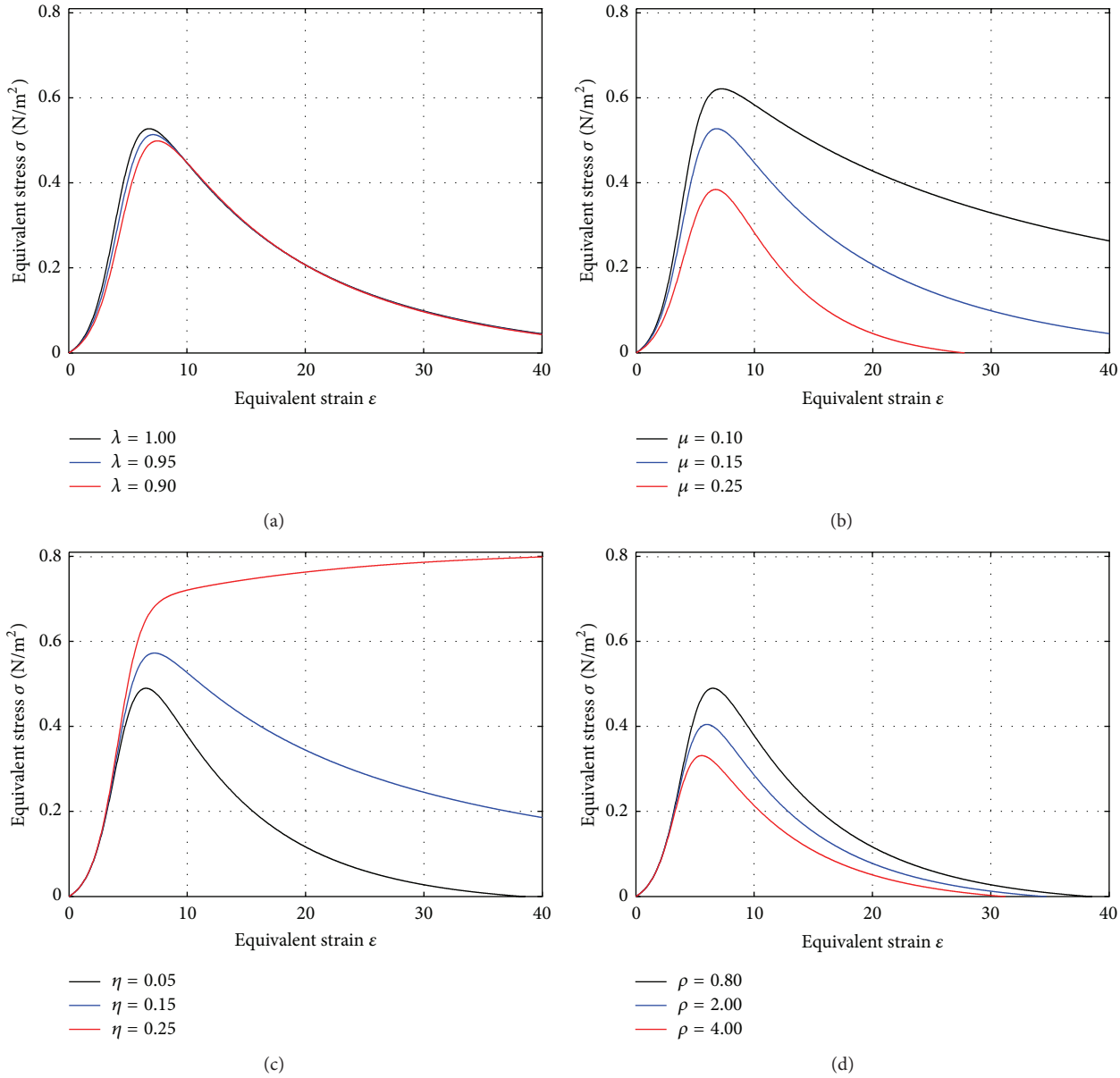

Figure 2: Numerical solutions of SIR for different parameter.

relative significance; it can be adjusted to a proportional coefficient to real physical value in practical applications.

3. Analytical Solution and Approximate Solution of SIR Model

The numerical solution of the SIR model is accurate but it must be calculated for any specific case, not representing the panorama and rule of the solution. Therefore, the analytical solution of the SIR model is necessary and it has important mathematical and mechanical meaning. Many corresponding studies of the analytical solution of the SIR model have been carried out, but the problem is not solved perfectly because the model has strong nonlinearity. There are some classic nonlinearity techniques that can be considered, such as Adomian decomposition method [9, 10], delta expansion method, and perturbation method [11, 12]. All these methods have some limitations, such that these techniques do not provide a convenient way to adjust and control the convergence region and rate of approximation series.

To overcome the mentioned limitations, Liao has proposed the homotopy analysis method (HAM) for nonlinear problems and then modified it step by step [13], and many nonlinear problems in different fields have been successfully solved by HAM.

Many problems such as boundary layer similarity solution for forced, natural, and mix convection in porous medium, heat transfer, and fluid mechanic problems are nonlinear inherently. The analytical solutions of nonlinear

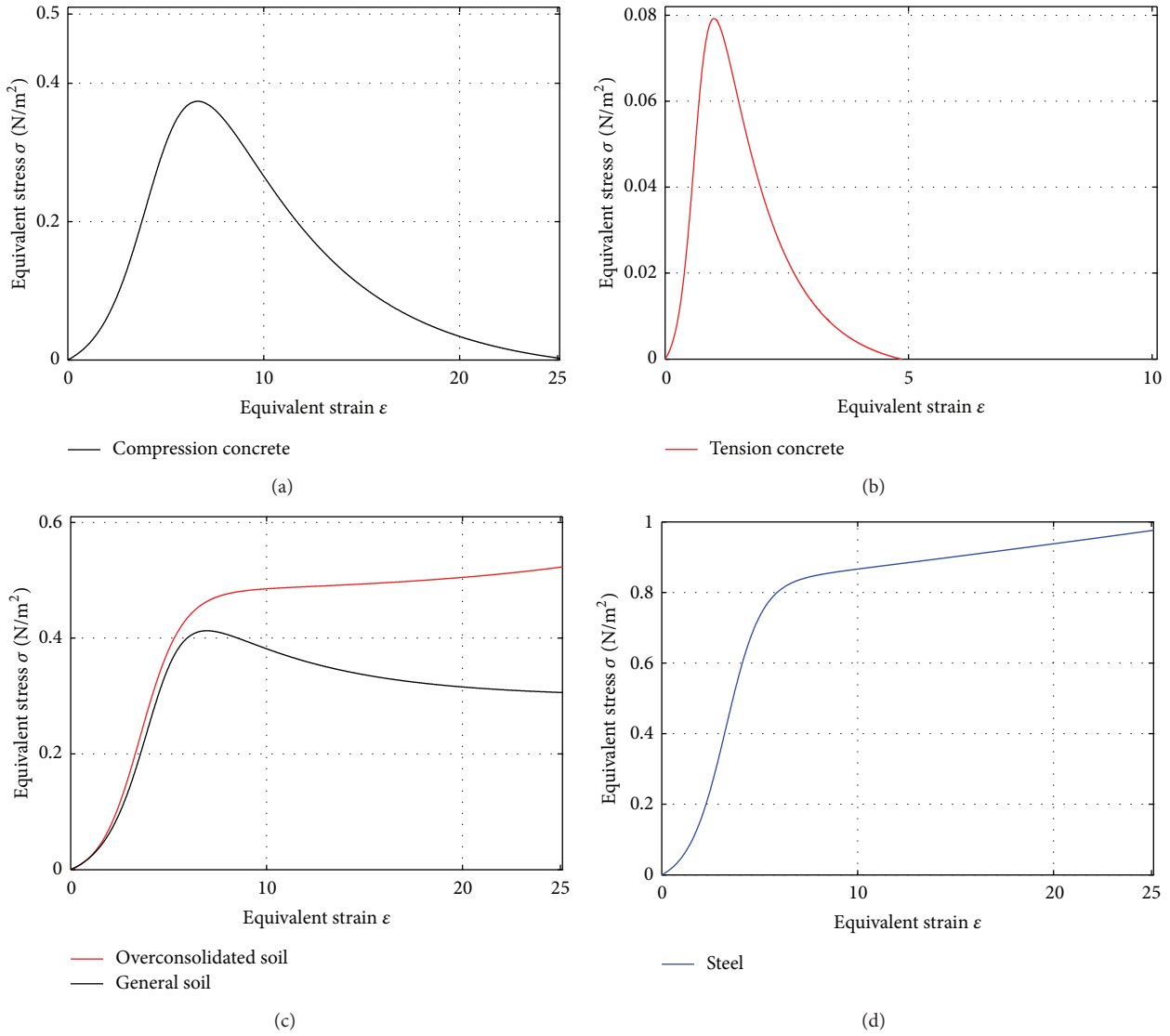

FIGURE 3: Constitutive curves for different engineering material based on SIR model.

ordinary differential equations can be solved by HAM [14–16].

HAM is based on homotopy, a concept in topology. The notion of equivalent maps or processes, where one can be deformed into the other, is the fundamental structure of homotopy. Two maps $f, g : X \to Y$ of topological spaces are homotopic if there exists a map $\phi : X \times I \to Y$ such that $\phi(x, 0) = f(x)$ and $\phi(x, 1) = g(x)$ for $x \in X$. Here, $X \times I$ denotes the product of X with unit interval $[0, 1]$ of real numbers. The map ϕ is called the homotopy between f and g. The basic idea of HAM is shown in the nonlinear differential equation as follows:

$$N\left[f\left(\vec{r}, t\right)\right] = 0, \tag{3}$$

where N is nonlinear operator, $\vec{r}$ is a vector of spatial variables, t denotes time, and $f(\vec{r}, t)$ is an unknown function. Boundary or initial conditions can be treated in a similar manner, which we avoid here just for simplicity [17].

Generalizing the concept of traditional homotopy, the so-called zero-order deformation equation is established as

$$\left(1 - q\right) L\left[\phi\left(\vec{r}, t; q\right) - f_0\left(t\right)\right] = q\hbar H\left(\vec{r}, t\right) N\left[\phi\left(\vec{r}, t; q\right)\right], \tag{4}$$

where $q \in [0, 1]$ is the embedding parameter, $\phi(\vec{r}, t; q)$ is an unknown function, $H(\vec{r}, t)$ is an auxiliary function, L is a linear operator, $f_0(t)$ is the initial guess, and $\hbar$ is a convergence-control parameter. As q increases from 0 to 1, $\phi(\vec{r}, t; q)$ vary from initial trial $f_0(t)$ to the exact solution $f(\vec{r}, t)$. If this variation is smooth enough, we construct the Maclaurin series of $\phi(\vec{r}, t; q)$ at $q = 0$ and the coefficients of all the higher terms can be obtained from the higher-order deformation equations. Differentiating the zeroth-order deformation equation above m times with respect to the embedding parameter q, then setting $q = 0$, and finally

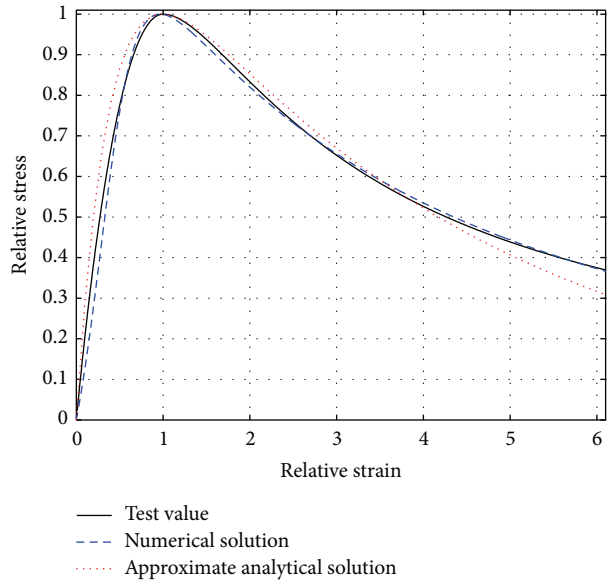

Figure 4: Concrete constitutive curves for different results.

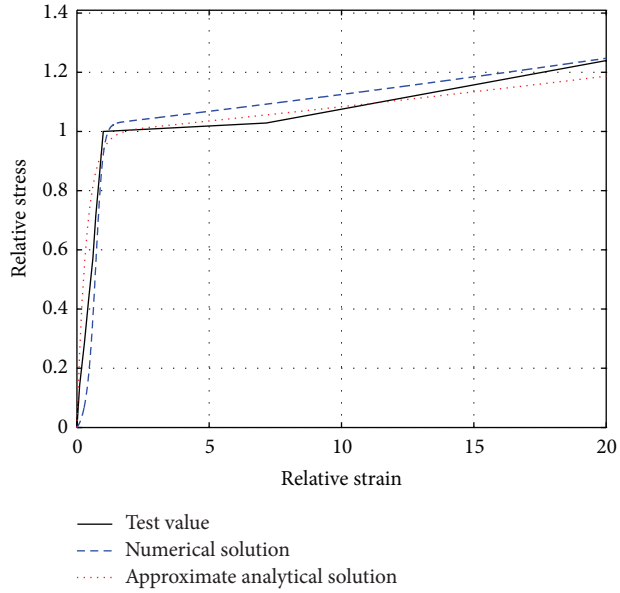

Figure 5: Steel constitutive curves for different results.

dividing by $m!$, we have the so-called mth-order deformation equations:

$$L\left[\phi_m\left(\vec{r},t;q\right)-\chi_m\phi_{m-1}\left(\vec{r},t;q\right)\right]=\hbar H\left(\vec{r},t\right)R_m \quad (5)$$

with $R_m=(\partial^m N[\phi(\vec{r},t;q)]/(m!\partial q^m))|_{q=0}=m!\cdot f_m(t)$.

In this way, a nonlinear equation is transformed into a series of linear equations. The exact solution of $f(\vec{r},t)$ is then approximated by the summation of the Maclaurin series at $q=1$. One has great freedom for the choice of linear operator L. For example, one can even select linear operator of different order as compared to the original nonlinear problem. To simplify the applications of HAM, Liao has suggested some rules, that is, the rule of solution expression, the rule of solution existence, and the rule of ergodicity for coefficients of homotopy series solution [13].

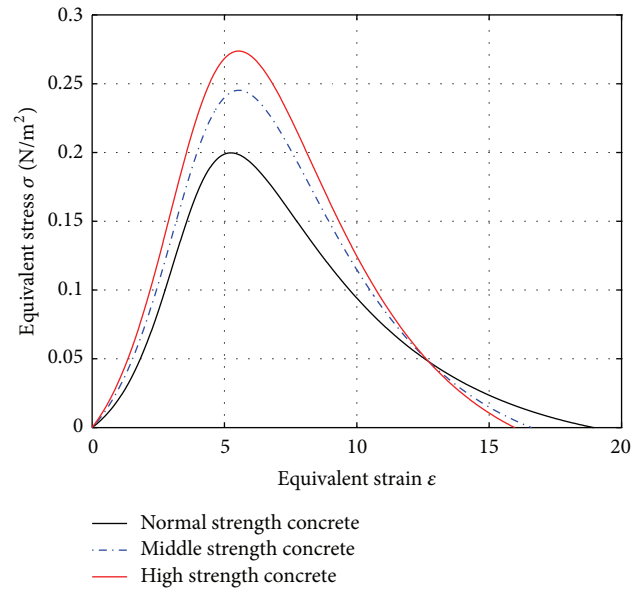

Figure 6: Constitutive curves for concrete based on SIR model.

In HAM, there is sufficient space for the convergence of the approximation by the introduction of $\hbar$ which greatly improves the early homotopy analysis method. It provides us with a simple way to ensure the convergence of the series solutions of nonlinear problems. This is an obvious advantage of HAM over homotopy perturbation method (HPM). In fact, HPM is just a special case of HAM when $\hbar=-1$, as pointed out by Liao and Abbasbandy and, in general, proved by Sajid and Hayat [18, 19]. Liao also has pointed out that HAM logically contains other nonperturbation methods such as Adomian's decomposition method [9], the δ-expansion method, and Lyapunov's artificial small parameter method [12].

From (2), we are led to define the two nonlinear operators as

$$\begin{aligned}&N_S\left[\sigma\left(\varepsilon;q\right),S\left(\varepsilon;q\right)\right]\\&\quad=\frac{\partial\sigma\left(\varepsilon;q\right)}{\partial\varepsilon}-\lambda\sigma\left(\varepsilon;q\right)S\left(\varepsilon;q\right)+\mu\sigma\left(\varepsilon;q\right),\\&N_I\left[\sigma\left(\varepsilon;q\right),S\left(\varepsilon;q\right)\right]\\&\quad=\frac{\partial S\left(\varepsilon;q\right)}{\partial\varepsilon}+\lambda\sigma\left(\varepsilon;q\right)S\left(\varepsilon;q\right)-\eta\sigma\left(\varepsilon;q\right)\\&\qquad+\rho\sigma^2\left(\varepsilon;q\right)S\left(\varepsilon;q\right).\end{aligned} \quad (6)$$

Let $s_0(\varepsilon)$ and $\sigma_0(\varepsilon)$ denote the initial guesses of $s(\varepsilon)$ and $\sigma(\varepsilon)$, L_S and L_σ the two auxiliary linear operators, $H_S(\varepsilon)$ and $H_\sigma(\varepsilon)$ the two auxiliary functions, and $\hbar$ an auxiliary parameter, all of which will be determined later. Let $q\in[0,1]$;

denote the embedding parameter. We construct the wroth-order deformation equations:

$$\begin{aligned}&(1-q)\,L_S\left[S(\varepsilon;q)-s_0(\varepsilon)\right]\\&\quad=q\hbar H_S(\varepsilon)\,N_S\left[S(\varepsilon;q),\sigma(\varepsilon;q)\right],\end{aligned}\tag{7}$$

$$\begin{aligned}&(1-q)\,L_\sigma\left[\sigma(\varepsilon;q)-\sigma_0(\varepsilon)\right]\\&\quad=q\hbar H_\sigma(\varepsilon)\,N_\sigma\left[S(\varepsilon;q),\sigma(\varepsilon;q)\right],\end{aligned}\tag{8}$$

subject to the initial conditions $S(0;q) = s(0)$ and $\sigma(0;q) = \sigma(0)$.

Expand $S(\varepsilon;q)$ and $\sigma(\varepsilon;q)$ in the Taylor series with respect to q; assuming that $H_S(\varepsilon)$ and $H_\sigma(\varepsilon)$ are properly chosen so that the above two series converge at $q = 1$, the solution series are

$$\begin{aligned}S(\varepsilon)&=s_0(\varepsilon)+\sum_{m=1}^{+\infty}s_m(\varepsilon),\\\sigma(\varepsilon)&=\sigma_0(\varepsilon)+\sum_{m=1}^{+\infty}\sigma_m(\varepsilon).\end{aligned}\tag{9}$$

Differentiating the wroth-order deformation equations (7) and (8) m times with respect to the embedding parameter q, then setting $q = 0$, and finally dividing by $m!$, the so-called mth-order deformation equations are

$$L_S\left[s_m(\varepsilon)-\chi_m s_{m-1}(\varepsilon)\right]=\hbar H_S(\varepsilon)\,R_m^S(\varepsilon),\tag{10}$$

$$L_\sigma\left[\sigma_m(\varepsilon)-\chi_m\sigma_{m-1}(\varepsilon)\right]=\hbar H_\sigma(\varepsilon)\,R_m^\sigma(\varepsilon),\tag{11}$$

subject to the initial conditions $\sigma_m(0) = 0$ and $s_m(0) = 0$, where $R_m^S(\varepsilon) = s'_{m-1}(\varepsilon) + \lambda\sum_{k=0}\sigma_k(\varepsilon)\,s_{m-1-k}(\varepsilon)$ and $R_m^\sigma(\varepsilon) = \sigma'_{m-1}(\varepsilon) + \mu\sigma_{m-1}(\varepsilon) - \lambda\sum_{k=0}\sigma_k(\varepsilon)s_{m-1-k}(\varepsilon)$. χ_m is 0 when m is not greater than 1, and χ_m is 1 in other cases.

Thus, $s(\varepsilon)$ and $\sigma(\varepsilon)$ can be expressed as

$$\begin{aligned}s(\varepsilon)&=s(\infty)+\sum_{k=1}^{+\infty}b_k e^{-k\beta\varepsilon},\\\sigma(\varepsilon)&=\sum_{k=1}^{+\infty}a_k e^{-k\beta\varepsilon}.\end{aligned}\tag{12}$$

From (1) and (2), $\sigma'(0) = \lambda\sigma(0)S(0) - \mu S(0)$ and $S'(0) = -\lambda\sigma(0)S(0) + \eta\sigma(0) - \rho\sigma^2(0)S(0)$. To obtain solutions in the form of (12), the initial guesses $s_0(\varepsilon)$ and $\sigma_0(\varepsilon)$ are expressed as follows:

$$s_0(\varepsilon)=s(\infty)+\gamma_{0,1}e^{-\beta\varepsilon}+\gamma_{0,2}e^{-2\beta\varepsilon},\tag{13}$$

where $\gamma_{0,1} = 2(s(0)-s(\infty)) - (\lambda s(0)+\rho s(0)i(0)-\eta)i(0)/\beta$ and $\gamma_{0,2} = s(\infty) - s(0) + (\lambda s(0)+\rho s(0)i(0)-\eta)i(0)/\beta$.

Consider

$$\sigma_0(\varepsilon)=\delta_{0,1}e^{-\beta\varepsilon}+\delta_{0,2}e^{-2\beta\varepsilon},\tag{14}$$

where $\delta_{0,1} = 2\sigma(0) + \sigma(0)(\lambda s(0) - \mu)/\beta$ and $\delta_{0,2} = -\sigma(0) - \sigma(0)(\lambda s(0) - \mu)/\beta$.

By choosing the auxiliary linear operators and from deformation equations and deformation derivative condition, we have

$$\begin{aligned}s_m(\varepsilon)&=\sum_{k=1}^{3m+2}\gamma_{m,k}e^{-k\beta\varepsilon},\\\sigma_m(\varepsilon)&=\sum_{k=1}^{3m+2}\delta_{m,k}e^{-k\beta\varepsilon},\end{aligned}\tag{15}$$

where $\delta_{m,k}$ and $\gamma_{m,k}$ are coefficients. Substituting the above expressions into (10) to (11), the recurrence formulas are

$$\begin{aligned}\delta_{m,1}&=-\sum_{j=2}^{3m+2}\delta_{m,j},\\\gamma_{m,1}&=-\sum_{j=2}^{3m+2}\gamma_{m,j},\\\delta_{m,j}&=\chi_m\chi_{3m-j+1}\delta_{m-1,j}-\left(\frac{\hbar}{\beta}\right)\frac{a_{m,j-1}}{j-1},\quad 2\le j<3m+2,\\\gamma_{m,j}&=\chi_m\chi_{3m-j+1}\gamma_{m-1,j}-\left(\frac{\hbar}{\beta}\right)\frac{b_{m,j-1}}{j-1},\quad 2\le j<3m+2,\end{aligned}\tag{16}$$

where a and b are parameters to meet deformation equation.

Finally, we get analytic solution of expressions in (2):

$$\begin{aligned}\sigma(\varepsilon)&=\sum_{m=1}^{+\infty}\sum_{k=1}^{3m+2}\delta_{m,k}e^{-k\beta\varepsilon},\\s(\varepsilon)&=s(0)+\sum_{m=1}^{+\infty}\sum_{k=1}^{3m+2}\gamma_{m,k}e^{-k\beta\varepsilon}.\end{aligned}\tag{17}$$

At this point, $\beta = \mu - \lambda s(\infty) \approx \mu$. According to the above conclusions and characteristics of solution, the approximate analytical solution of (17) can be expressed as

$$\sigma(\varepsilon)=\sum_{i=1}^{n}(-1)^{i+1}c_i e^{-k_i\mu\varepsilon},\tag{18}$$

where n belongs to even number and $c_i = c_{i+1}$ when i is an odd number. The above approximate analytical solution can usually achieve adequate satisfactory results when n is 2 or 4. As a simplified format, the equation above can also be transformed as follows:

$$\sigma(\varepsilon)=c_1\left(e^{-k_1\mu\varepsilon}-e^{-k_2\mu\varepsilon}\right).\tag{19}$$

The comparison of the real concrete strain-stress curve, the numerical solution curve, and the approximate analytical solution of the SIR model is shown as Figure 4, and the comparison of steel is shown in Figure 5. It can be seen that both the numerical solution and the approximate analytical solution fit the original value precisely. It is worth noting that the approximate analytical solution reflects the

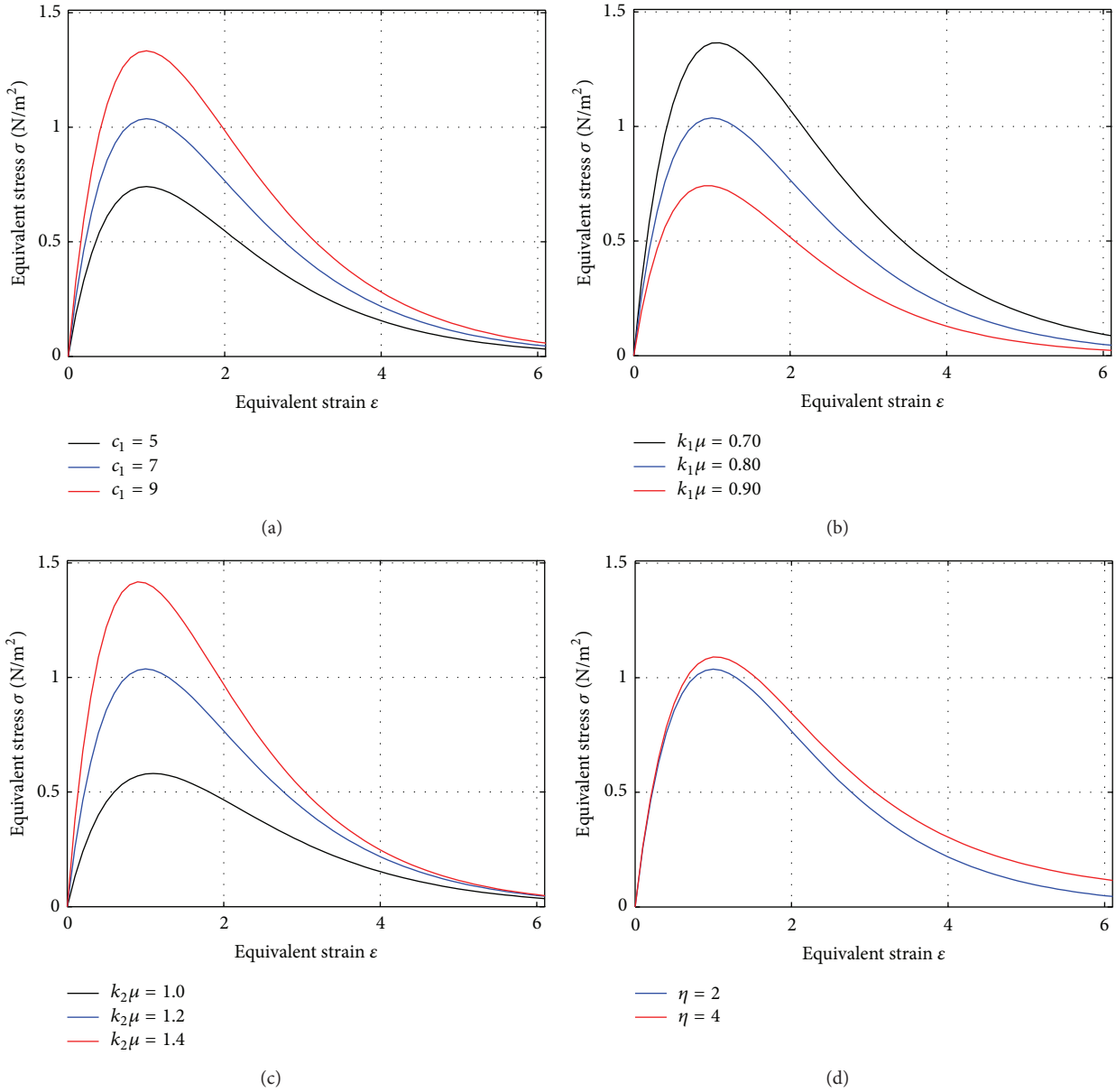

Figure 7: Approximate solutions based on SIR model with different parameter.

connotation and characteristics of the analytical solutions, but it nevertheless has a certain similarity, and the specific value of c_i in the solution should be adjusted appropriately according to actual condition and the numerical solution in order to obtain better accuracy. In addition, Umemura and Aoyama [20] have presented an exponential constitutive relation for concrete, which is similar with the model as (18) in n equals 2. However, the original exponential relation is determined by experimental data fitting, and the proposed solution in this paper has the theoretical basis and generality; the results can be verified with each other. The effect of various parameters in (18) on solutions is shown in Figure 7. The stress-strain curve of compression concrete with different strength is shown as Figure 8, and the simulation curves are similar with the experimental data in shapes and the variation rules, indicating that the approximate analytical solution put forward in this paper can also embody the intrinsic characteristics and variation of the SIR model.

4. Size Effect and Strain Rate Based on SIR Solution

For real engineering materials, the mechanical properties also related to size, load mode, and external environment besides their own composition and characteristics and mainly include size effects, strain rate, and multiaxis loading. In this paper, the uniaxial stress-strain curve on the influence of size effect and strain rate of are mainly discussed.

The size effect of material strength refers to phenomenon that large size member in brittle material usually fractures

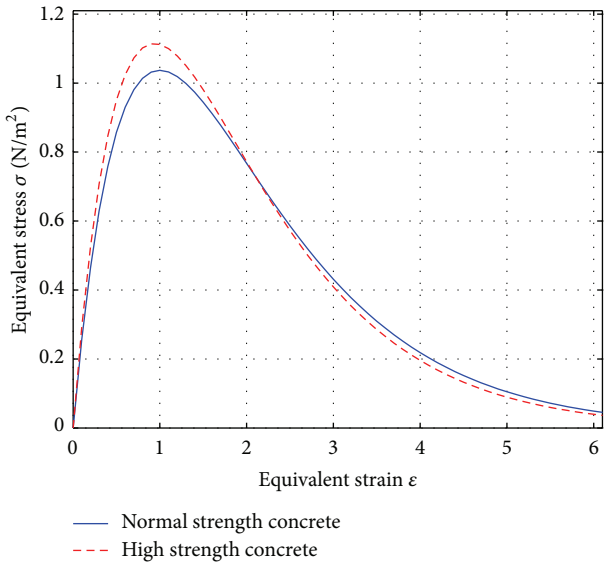

FIGURE 8: Constitutive relation of concrete with different strength based on approximate solutions.

under a lower nominal stress than geometrically similar small-size member (the nominal stress being defined as the load divided by the characteristic cross section area). Early researchers suppose that any observed size effect should be described by extreme value statistics prevailed in structural engineering. In the mid 1970s, the fact that there exists a purely deterministic size effect, caused by energy release associated with stress redistribution prior to failure and that this energetic size effect usually dominates in the so-called quasibrittle structures (i.e., structures in which fracture propagation is preceded by a relatively large fracture process zone which, in contrast to brittle ductile fracture of metals, exhibits almost no plastic deformations but undergoes progressive softening due to microcracks) gradually emerged.

Bažant and Chen [21] and Bažant and Planas [22] summarized six main causations for size effect which include boundary layer, diffusion phenomena, hydration heat, randomness of material strength, energy release, and the fractal character of the crack surface. Recent research focuses on three main types of size effects, namely, the statistical size effect due to randomness of strength, the energy release size effect, and the possible size effect due to fractality of fracture or microcracks.

Recent research has shown that the elastic modulus and the peak stress of brittle material will gradually decrease with the increase of the member size and depth-width ratio; at the same time, the strain value at the peak stress changes a little, and the descent rate of stress and fragility at the softening section will also reduce [23], as shown in Figures 2 and 7. In some cases, the curves of different sizes in softening section can even intersect as shown in Figures 6 and 8.

In fact, for the large size member with the same axial force, the total number and size of microcracks are bigger and the domain that the sustained damage occurs is larger. Hence, the equivalent strain energy for damage needs fewer paths and the damage propagation needs shorter paths, which lead to the probability of regional brittle failure; that is, the failure rate in unit and its growth rate both increase.

Considering the above characteristic of size effect, the SIR model can simulate the size effect of brittle material and the whole process of failure. The advantage of the application of the SIR model is the physical significance being explicit and the variation can be realized by enhancing the failure rate in unit μ and the reduced speed parameter for invalid elements due to stress transmission and distribution ρ, referring to Figure 2.

The materials such as concrete and rocks are typical rate sensitive for their strength, ductility, and failure mode will significantly change in different strain rates. Existing research shows that the elastic modulus and the ultimate strength of rate sensitive material will enhance with increasing strain rate, and the strain value at the peak stress changes a little [23]. In different strain rates, the stress-strain full curve of concrete is basically consistent with the whole curve under static load in shape; however, the ductility increases slightly, as shown in Figures 2 and 7.

For the materials subjected to the same axial force, if the strain rate increased, the internal microcracks in the mortar substrate are late to fully extent, but the quantity and degree of the damaged aggregate relatively increase which lead to the enhancement of the failure strength. At the same time, the unit failure rate increased, and the increase rate of the stressed unit sustainably grows.

Therefore, the SIR model can show the influence of the strain rate from the physical sense by properly adjusting parameters, and the simulation is realized by enhancing the failure rate μ and the increase rate of stressed units when the invalid units grow η, referring to Figure 2.

The above discussion illustrates the direct relationship between size effect, strain rate, and the SIR model with its numerical solution from mechanical principle and propagation characteristic. In practical applications, the approximate analytic solution of the model is more convenient, so the study below will discuss the adjustment of coefficient c_i in the approximate analytic solution for the purpose of representing size effect and strain rate.

The most widely used theory is the size effect law proposed by Bažant and Chen [21] based on a large number of experiments, and this method put forward the size effect unified formula in certain extent according to plasticity theory or elastic theory:

$$\frac{\sigma_N}{f_c} = \frac{B}{\sqrt{1 + (D/D_0)}}, \tag{20}$$

where σ_N is the nominal stress when material is damaged, B is dimensionless parameter, f_c is the strength of the quasi brittle material, D is the characteristic length of the structure, and D_0 is the constant related to structural shape. It can be seen from Figure 6 that the consideration about size effect can be realized by modulating c_i and k_i properly in the approximate analytical solution of SIR.

In the usual study, the strain rate effect coefficient of compression concrete is described as the following exponential form according to European standard [24]:

$$\frac{\sigma_{cd}}{\sigma_{cs}} = \left(\frac{\dot{\varepsilon}}{\dot{\varepsilon}_0}\right)^{1.026\alpha}, \quad \dot{\varepsilon} \le 30/\mathrm{s},$$
$$\frac{\sigma_{cd}}{\sigma_{cs}} = \gamma_s\left(\frac{\dot{\varepsilon}}{\dot{\varepsilon}_0}\right)^{1/3}, \quad \dot{\varepsilon} > 30/\mathrm{s}, \tag{21}$$

where $\dot{\varepsilon}$ is the current material strain rate, $\dot{\varepsilon}_0$ is the quasi static strain rate, taken as 3×10^{-5}/s, and σ_{cs} and σ_{cd} are the static and dynamic compression strength of concrete, respectively. One has $\alpha = 1/(5 + 0.9\,\sigma_{cs})$ and $\log \gamma_s = 6.156\,\alpha - 2$.

For tensioned concrete

$$\frac{\sigma_{td}}{\sigma_{ts}} = \left(\frac{\dot{\varepsilon}}{\dot{\varepsilon}_0}\right)^{1.016\delta}, \quad \dot{\varepsilon} \le 30/\mathrm{s},$$
$$\frac{\sigma_{td}}{\sigma_{ts}} = \beta\left(\frac{\dot{\varepsilon}}{\dot{\varepsilon}_0}\right)^{1/3}, \quad \dot{\varepsilon} > 30/\mathrm{s}, \tag{22}$$

where $\dot{\varepsilon}$ is the current material strain rate and $\dot{\varepsilon}_0$ is the quasi static strain rate, taken as 3×10^{-5}/s, and σ_{cs} and σ_{cd} are the static and dynamic tension strength of concrete, respectively. One has $\delta = 1/(10 + 0.6)\,\sigma_{ts}$ and $\log \beta = 7.11\delta - 2.33$.

The strain rate effect coefficient of steel I is as follows:

$$\frac{f_{yd}}{f_{ys}} = \left(1 + \frac{d_1}{f_{ys}\ln\left(\dot{\varepsilon}/\dot{\varepsilon}_0\right)}\right)$$
$$\frac{f_{ud}}{f_{us}} = \left(1 + \frac{d_2}{f_{us}\ln\left(\dot{\varepsilon}/\dot{\varepsilon}_0\right)}\right), \tag{23}$$

where $\dot{\varepsilon}$ is the current material strain rate and $\dot{\varepsilon}_0$ is the quasi static strain rate, taken as 3×10^{-4}/s, and f_{ys} and f_{yd} are the static and dynamic strength, respectively. d_1 and d_2 are the test parameters obtained by regression analysis method [25, 26].

Referring to Figure 7, the strain rate effects on concrete can be simulated by modulating c_i and k_i properly for the approximate analytical solution of SIR model. In addition, if k_i is taken as a small negative number when i is an odd, the characteristics of strengthening after yielding for metal materials can also be simulated, and the stress-strain curve of metal with high strain rate or high strength can be obtained by enlarging the absolute value of c_i or k_i, as shown in Figure 9.

In conclusion, it is significant that the coefficient c_i of the approximate analytical solution implies the multiple parameters interaction in SIR model, and the size effect and strain rate in the whole load process can be achieved by regulating c_i. The factor ζ_s on size effect can be achieved from (19) and the factor ζ_d on strain rate can be achieved from (21) to (23). Thus, the correction coefficient about c_i is

$$c_{ic} = \left(k_s\zeta_s + k_d\zeta_d\right)c_i, \tag{24}$$

where k_s and k_d are adjustment coefficient on size effect and strain rate, respectively, and the more precise value should be determined by experimental data.

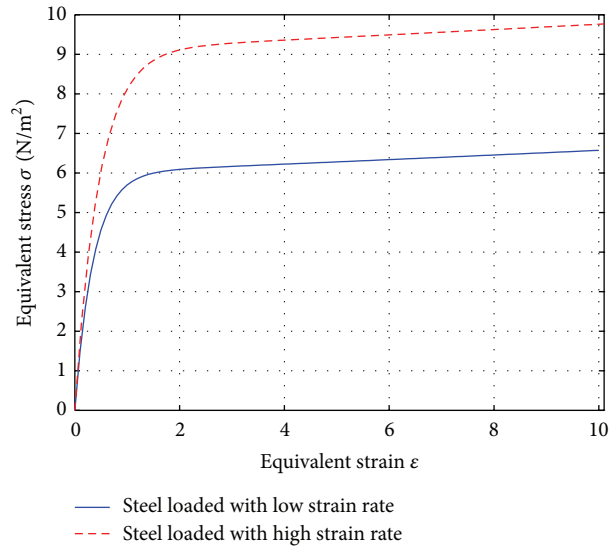

Figure 9: Constitutive relation of steels with different strain rate based on approximate solutions.

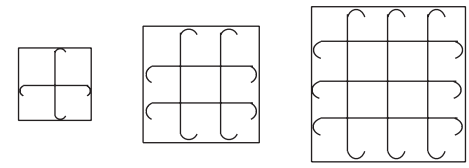

Figure 10: Configurations of stirrups.

5. Test on the Size Effect of Confined Concrete

As mentioned above, the uniaxial construction relationship of single material based on SIR model and HAM method is presented. However, the normal member of civil engineering consists of both concrete and steel, and the constructive relationship of reinforced concrete and confined concrete and corresponding properties such as size effect need more research.

In order to verify the feasibility of the construction relationship for confined concrete based on the SIR model, six reinforced concrete prism specimens confined by square stirrups were made. Each type of specimen contains two same members, and the volumetric percentage of stirrups is 1.26% for all. The configurations of stirrups are shown in Figure 10. The design parameters of the specimens are listed in Table 1. For the concrete used, the normal prismatic compressive strength is 42.67 N/mm^2, the ultimate compression strain is 0.0022, and Young's modulus is 3.08×10^4 N/mm^2. For the steel bars, the average yield strength is 480 N/mm^2, the ultimate strength is 665 N/mm^2, and Young's modulus is 2.05×10^5 N/mm^2.

The electrohydraulic servo testing machine with 4×10^4 kN maximum range was used as the load device and the continuous axial monotonic load was applied, as shown in Figure 11. When the force is less than the ultimate bearing

Figure 11: Loading and measuring instruments.

Figure 12: Final failure mode of specimens.

Table 1: Design parameters of the specimens.

Parameters (unit)	Notation	Specimen size		
		Small	Middle	Large
B (mm)	Section length	400	600	800
H (mm)	Height of specimen	1200	1800	2400
d_s (mm)	Diameter of stirrups	10	12	14
s (mm)	Spacing of stirrups	103	132	169
c (mm)	Thickness of protective layer	20	30	40
d_l (mm)	Diameter of longitudinal bars	12	18	22

capacity, the load was controlled by force and then by displacement. The measured parameters include axial loads, axial deformation, and stirrups strain. The final failure modes of specimens are shown in Figure 12.

The axial load value is measured by the strain force transducer with 1×10^4 kN measuring range. The axial compression is measured by the displacement meter with 200 mm measuring range and the gauge length is 2/3 of the specimen height. The average stress-strain relation of cross section curves of the specimens with different sizes is shown in Figure 13. The abscissa ε is obtained by the measured displacement divided by the respective gauge length. Ordinate σ is the relative stress, equal to the axial load value divided by the cross-sectional area of the specimen.

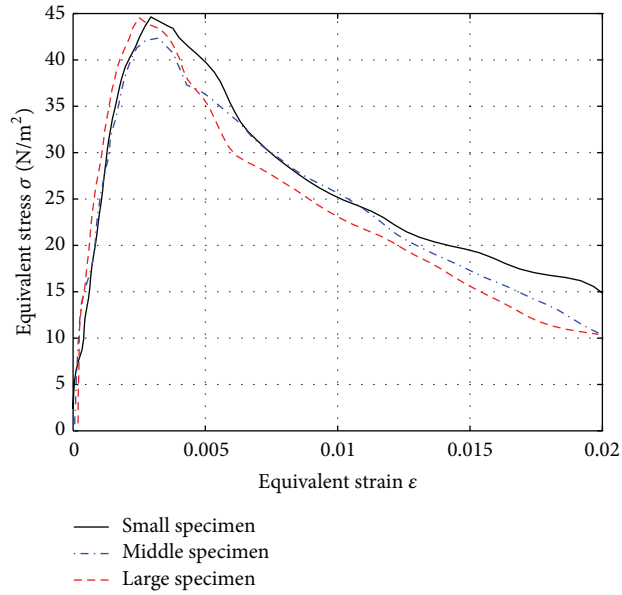

Figure 13: Stress-strain curve of gross area for all prism specimens.

Table 2: Parameters of the approximate solution.

c_1	k_1	k_2
1.345	2.305	20.546
1.386	2.727	23.785
1.391	3.119	28.267

According to the stress-strain relation of the specimens with different sizes, the approximate solution based on nonlinear data fitting and (19) is presented as shown in Figure 14. The failure rate μ is assumed as 0.1, and the parameters in (19) are listed in Table 2. It is significant that the curves of the approximate solution fit well with the original data and the variation trend and the variance rule among the curves are clearly revealed. The SIR model and the corresponding approximate solution are suitable for confined concrete and complex composite material with size effect.

6. Conclusion

Though there are various constitutive relation models of engineering material at present, the united constitutive relation model is rare and it is necessary to establish a model which can present many properties in different materials by concise form.

Under the external load, the member composed of engineering materials is damaged inevitably and the damage

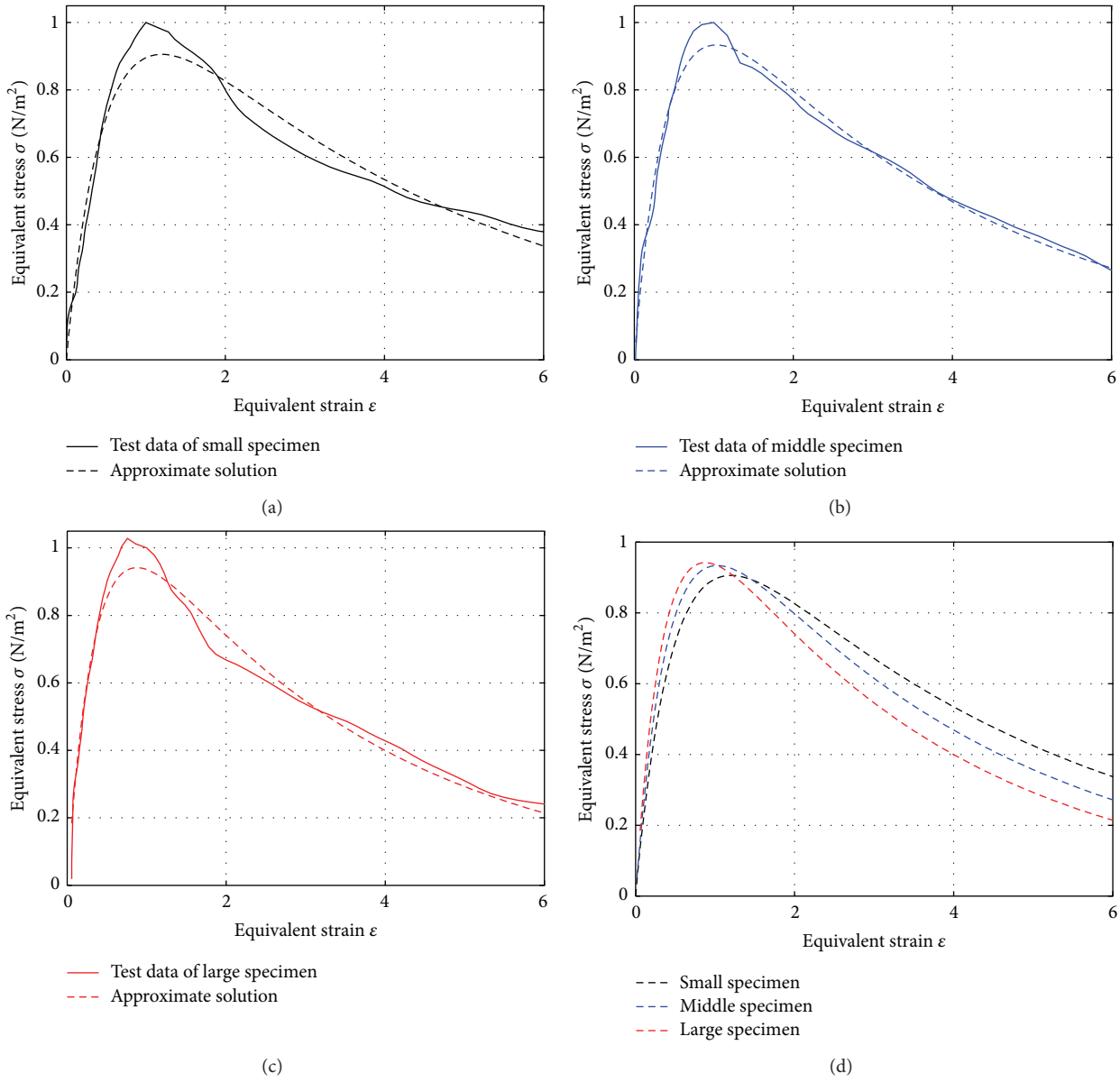

Figure 14: Stress-strain curve comparison of test value and approximate solution.

will propagate in the units and the system. This phenomenon has similar rule as the infectious disease. During infectious disease, the population includes the Susceptible people, the Infected people, and the Removal people. The SIR model originates from the infectious disease transmission dynamics and the complex system of population, which reflects the dynamic characteristics and the transmit laws of different parts of the system under the action of external factors and patterns. Hence, the SIR model can be used for reference and to indicate the full stress-strain curve in uniaxial material with high precision. The numerical results show that the constitutive relation in different materials can be simulated by choosing appropriate parameters in the SIR equations.

In this paper, the SIR models are described by coupled nonlinear differential equations, and the analytic solution form and approximate analytic solution of SIR model are obtained by means of an analytic technique for nonlinear problems, namely, the homotopy analysis method (HAM). According to the different solutions on the variation of the parameters in the SIR model, the mechanical characteristics of various materials are compared and the factors of the size effect and the strain rate are discussed. The results show that the SIR model and its solution presented in this paper have versatility and can provide unified constitutive relations for a variety of engineering materials.

However, the SIR model only has an implicit form, which differs with the traditional constitutive relations established by experimental results, damage mechanics, and fracture mechanics, and the intension and laws need further study. Furthermore, the SIR model and its solution are merely

suitable for the materials under uniaxial load. The models for materials under multiaxial load and fatigue load are necessary to be developed and discussed.

Conflict of Interests

The authors declare that there is no conflict of interests regarding the publication of this paper.

Acknowledgments

This work is partially supported by the Natural Science Foundation of China under Grant nos. 51108009 and 50878010, the Foundation of the Ministry of Education of China for Outstanding Young Teachers in University under Grant no. 20111103120022, and the Foundation of Beijing Key Lab of Earthquake Engineering and Structural Retrofit under Grant no. 2013TS02.

References

[1] R. K. Rajput, *Engineering Materials*, Chand and Company Ltd., New Delhi, India, 2008.

[2] W. F. Chen, *Plasticity in Reinforced Concrete*, J. Ross Publishing, Fort Lauderdale, Fla, USA, 2007.

[3] F. Lene, "Damage constitutive relations for composite materials," *Engineering Fracture Mechanics*, vol. 25, no. 5-6, pp. 713–728, 1986.

[4] N. Burlion, F. Gatuingt, G. Pijaudier-Cabot, and L. Daudeville, "Compaction and tensile damage in concrete: constitutive modelling and application to dynamics," *Computer Methods in Applied Mechanics and Engineering*, vol. 183, no. 3-4, pp. 291–308, 2000.

[5] W. O. Kermack and A. G. McKendrick, "Contribution to the mathematical theory of epidemics," *Proceedings of the Royal Society of London A*, vol. 115, pp. 700–721, 1927.

[6] H. W. Hethcote, "The mathematics of infectious diseases," *SIAM Review*, vol. 42, no. 4, pp. 599–653, 2000.

[7] Z. M. Wang, A. K. H. Kwan, and H. C. Chan, "Mesoscopic study of concrete I: generation of random aggregate structure and finite element mesh," *Computers and Structures*, vol. 70, no. 5, pp. 533–544, 1999.

[8] P. Wriggers and S. O. Moftah, "Mesoscale models for concrete: homogenisation and damage behaviour," *Finite Elements in Analysis and Design*, vol. 42, no. 7, pp. 623–636, 2006.

[9] G. Adomian, "Nonlinear stochastic differential equations," *Journal of Mathematical Analysis and Applications*, vol. 55, no. 2, pp. 441–452, 1976.

[10] G. Adomian, *Solving Frontier Problems of Physics: The Decomposition Method*, Kluwer Academic Publishers, Boston, Mass, USA, 1994.

[11] J. D. Cole, *Perturbation Methods in Applied Mathematics*, Blaisdell Publication Company, Waltham, Mass, USA, 1968.

[12] A. H. Nayfeh, *Perturbation Methods*, Wiley-Interscience, New York, NY, USA, 2000.

[13] S. Liao, *Beyond Perturbation: Introduction to the Homotopy Analysis Method*, Chapman & Hall, Boca Raton, Fla, USA, 2003.

[14] A. R. Sohouli, D. Domairry, M. Famouri, and A. Mohsenzadeh, "Analytical solution of natural convection of Darcian fluid about a vertical full cone embedded in porous media prescribed wall temperature by means of HAM," *International Communications in Heat and Mass Transfer*, vol. 35, no. 10, pp. 1380–1384, 2008.

[15] Z. Ziabakhsh and G. Domairry, "Solution of the laminar viscous flow in a semi-porous channel in the presence of a uniform magnetic field by using the homotopy analysis method," *Communications in Nonlinear Science and Numerical Simulation*, vol. 14, no. 4, pp. 1284–1294, 2009.

[16] A. Kargar and M. Akbarzade, "Analytic solution of natural convection flow of a non-newtonian fluid between two vertical flat plates using homotopy perturbation method (HPM)," *World Applied Sciences Journal*, vol. 20, no. 11, pp. 1459–1465, 2012.

[17] S. Liao and Y. Tan, "A general approach to obtain series solutions of nonlinear differential equations," *Studies in Applied Mathematics*, vol. 119, no. 4, pp. 297–354, 2007.

[18] S. Abbasbandy, "The application of homotopy analysis method to nonlinear equations arising in heat transfer," *Physics Letters A*, vol. 360, no. 1, pp. 109–113, 2006.

[19] M. Sajid and T. Hayat, "Comparison of HAM and HPM methods in nonlinear heat conduction and convection equations," *Nonlinear Analysis. Real World Applications*, vol. 9, no. 5, pp. 2296–2301, 2008.

[20] H. Umemura and H. M. T. Aoyama, *Experimental Studies on Reinforced Concrete Members and Composite Steel and Reinforced Concrete Members*, University of Tokyo Publication, Tokyo, Japan, 1970.

[21] Z. P. Bažant and E. P. Chen, "Scaling of structural failure," *ASME Applied Mechanics Reviews*, vol. 50, pp. 593–627, 1997.

[22] Z. P. Bažant and J. Planas, *Fracture and Size Effect in Concrete and Other Quasibrittle Materials*, CRC Press, Boca Raton, Fla, USA, 1998.

[23] L. J. Malvar and C. A. Ross, "Review of strain rate effects for concrete in tension," *ACI Materials Journal*, vol. 95, no. 6, pp. 735–739, 1998.

[24] Comite Euro-International du beton, *CEB-FIP Model Code 1990*, Wiltshire Redwood Books, Trowbridge, UK, 1993.

[25] I. Rohr, H. Nahme, and K. Thoma, "Material characterization and constitutive modelling of ductile high strength steel for a wide range of strain rates," *International Journal of Impact Engineering*, vol. 31, no. 4, pp. 401–433, 2005.

[26] F. Lin, X. L. Gu, X. X. Kuang, and X. J. Yin, "Constitutive models for reinforcing steel bars under high strain rates," *Journal of Building Materials*, vol. 11, no. 1, pp. 14–20, 2008.